Rev. Roum. Sci. Techn.– Électrotechn. et Énerg.
Vol. **67**, *3*, pp. 247–252, Bucarest, 2022

ALTERNATIVE HYBRID CONTROL OF SWITCHED SYSTEMS. AN APPLICATION TO DC MACHINE FED BY MULTICELLULAR CONVERTER

IBRAHIM BENTCHIKOU[1], KHALED HALBAOUI[2], FARES BOUDJEMA[3], DJAMEL BOUKHETALA[3], TLEMÇANI ABDELHALIM[4]

Keywords: Hybrid control; Floating condensers; Multicellular converter.

In this article, we present an alternative of hybrid control, where we choose as an actuator the dc motor controlled by a multi-cellular converter. For this, a switching control for the multi-cellular converter is established to provide the proper reference value for regulating the speed by using the Petri nets. We consider a converter with three cells represented as a hybrid system with eight modes of operation. The operation modes of the system are governed by the adjustable reference voltage and reference speed, which are calculated using an energy balance principle. Simulation results are given to illustrate the performance of such a method. To show the validity of our approach, a practical implementation based on Spartan 3E FPGA resulted.

1. **INTRODUCTION**

Many approaches from continuous automatic dynamical systems have been applied to classes of hybrid systems. Branicky and al. [1] proposed algorithms for finding an optimal trajectory for the control of SDH. They are based on the resolution of the equation of Hamilton-Jacobi-Bellman, which is the result of previous developments in dynamic programming theory on discrete Automatic Event Systems and the extension of the Hamilton-Jacobi equation for continuous-times systems. Other work has been done to extend the principle of a maximum of Pontryagin, by SDH [2]. In [3], this approach has been exploited for a process of a mixture of products. For hybrid systems of hysteresis type, a numerical optimization method for calculating an optimal control performing under constrained trajectory tracking has been used in [4]. This method is applied to a temperature control system controlled by a thermostat.

Another alternative is extending the classic predictive control to the SDH, proposed by Bemporad in [5]. The implementation of this command requires the solution of a mixed quadratic programming problem, the resolution of an optimization problem including a quadratic cost function, where the optimization vector is composed of mixed variables (continuous, binary), and linear constraints. This technique was applied to a process in three reservoirs [6]. In 1987 the authors adopted the approach of Bemporad to overcome the problem related to the complexity of the calculation. A genetic algorithm-based control strategy is presented to reduce the computation time. The comparative study between this strategy and the one proposed in [5], performed on a three-tank test bench, shows that the calculation time at the beginning has been reduced by about two minutes per iteration. The second strategy is more effective when the prediction horizons are great. All these methods have a computational complexity that generally requires a considerable computation time, which reduces their scope of application for slow processes such as chemical or thermal processes. For example, applications that interest us are situated primarily in the field of electromechanical whose electrical values are rapidly evolving, and implementation in real-time of these controls is not envisaged. This constraint has led us to suggest a control that may consider the time constraints of execution, material, and processing power and leads to a procedure of simple and efficient implementation.

In this article, we have proposed an alternative for the control of switching systems using multicellular converters to feed the load that is, in our case, the dc machine. We noticed that the structure of this type of converter lends itself naturally to hybrid modeling due to the natural presence of continuous and discrete variables. We saw that the operation of this system by using the model of the various modes by choosing a law of commutation and imposing conditions of transition ensures the safety and stability of the multicellular converter. This control requires knowledge at any moment of the measurement of the floating voltage and motor speed.

An electromechanical system must be ruled by the following equation [3].

$$[S] = [P]\cdot[A]\cdot[C]\,, \tag{1}$$

where S is the electro-mechanical system; P is the power supply; A the actuator, and C is the control. Hence, to make the system work at its optimum and run under the most efficient ability, the parameters of the equations must meet the following criteria:

$$[S]_T = [P]_P\cdot[A]_S\cdot[C] \tag{2}$$

construct a system that works at the optimal status and in very favorable conditions, *i.e.*, which tends towards the ideal, we must construct a highly reliable actuator with a good yield, good stability, a perfect power supply, and robust control. We need to add the third term so that it operates the system in a closed loop. We explain the three terms of equation (2) in detail.

[1] Intelligent Systems Laboratory (LESI) of the University of Khemis Miliana, Ain Defla, Algeria; Email, b.bentchikou@univ-dbkm.dz
[2] Centre de Recherche Nucleaire de Birine Ain oussera, Laboratoire d'Electronique de Puissance & Commande, Algeria; Email : halbaoui_khaled@yahoo.fr
[3] Laboratory of Process Control, National Polytechnic School, ENP, Algeria; Email: fares.boudjema@enp.edu.dz djamel.boukhetala@g.enp.edu.dz
[4] Research Laboratory in Electrical Engineering and Automatic (LREA), Medea, Algeria: Email, h_tlemcani@yahoo.fr

2. SYSTEM ELECTRO-MECHANICAL

Our actuator, $[A]$, is a dc motor, the engine used until now because it has become indispensable in some applications. These motors still have many practical applications, such as automotive, aircraft, portable electronic devices, and speed control applications.

An advantage of dc motors is that it is easy to control their speed in a wide diapason.

3. THE POWER SUPPLY STUDY

Power electronics is an important technological development thanks to the development of semiconductor power and new energy conversion systems [5, 7]. The idea of multicellular converters first appeared in the 1990s [5, 9], and it proposed a series of elementary commutation cells linked with floating multicellular converter's voltage sources. This allowed the distribution of high voltages over more switching elements and, therefore, the ability to use switching components with lower constraints and better performances [5]. The power supply [P] is represented here by a four-level three-cell dc/dc converter. Its function is to split the supply voltage and distribute it in smaller values on several levels [6, 10, 11]. Therefore, a good approximation of a particular waveform can be obtained. Figure 1 shows a four-level three cells converter whose function is to feed a dc machine.

3.1. MODELING OF THE MULTICELLULAR CONVERTER.

The modeling of multicellular converters is generally difficult. Indeed, it contains continuous variables (voltages and currents) and discrete variables (switches, or a discreet location) [12, 13]. The multicell converter contains several cells. Each cell contains two complementary electronic power components and can be controlled by a binary switch UK. This switch equals 1 when the upper switch of the cell is conducting and 0 when the lower complementary switch of the cell is conducting. These cells are serially associated with the charge and separated by capacities [12].

At the output, one obtains (p+1) levels (0, E/p,…,(p–1) E/P, E). This association in series allows the output source V_s to evolve on p possible levels.

Thus, it is necessary to ensure an equilibrated distribution of the voltage of the floating condensers. Under these conditions, one obtains the following property: The inverter has p –1 floating voltage sources, and the voltage of the capacity of index k is kE/p [5].

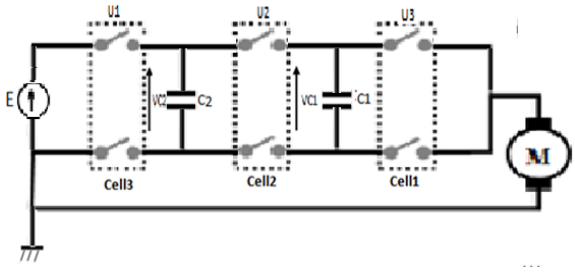

Fig. 1 – Multicellular converter with 3 cells and a dc machine load.

To simplify the study and notations, we will study the operation and behavior of a converter with 3 cells. For this, the following differential equations describe our system (converter-load)

$$\begin{aligned}
\frac{\mathrm{d}v_{c1}}{\mathrm{d}t} &= \frac{1}{c_1}(u_2-u_1)i,\\
\frac{\mathrm{d}v_{c2}}{\mathrm{d}t} &= \frac{1}{c_2}(u_3-u_2)i,\\
\frac{\mathrm{d}i}{\mathrm{d}t} &= -\frac{R}{L}i+\frac{E}{L}u_3-\frac{v_{c2}}{L}(u_3-u_2)-\frac{v_{c1}}{L}(u_2-u_1)-\frac{K_e}{L}w,\\
\frac{\mathrm{d}w}{\mathrm{d}t} &= \frac{K_c}{J_m}i-\frac{f_m}{J_m}w-\frac{C_r}{J_m}.
\end{aligned} \tag{3}$$

From eq. (3) we can define the state equation of this system:

$$\begin{bmatrix}\dot{v}_{c1}\\ \dot{v}_{c2}\\ \dot{I}\\ \dot{w}\end{bmatrix}=\begin{bmatrix}0 & 0 & \frac{u_2-u_1}{C_1} & 0\\ 0 & 0 & \frac{u_2-u_1}{C_2} & 0\\ \frac{u_2-u_1}{L} & \frac{u_2-u_1}{L} & \frac{-R}{L} & \frac{-K_e}{L}\\ 0 & 0 & \frac{K_c}{J_m} & \frac{-f_m}{J_m}\end{bmatrix}\cdot\begin{bmatrix}v_{c1}\\ v_{c2}\\ I\\ w\end{bmatrix}+\begin{bmatrix}0\\ 0\\ \left(\frac{E}{L}\right)u_2\\ -C_r/j_m\end{bmatrix}. \tag{4}$$

4. HYBRID AUTOMATA-BASED MODELING AND DESIGN CONTROL

Hybrid automata are dynamic systems that describe the evolution in time of the values of a set of discrete and continuous state variables. The hybrid system is described by the interaction between a continuous dynamical system, whose behavior is characterized by continuous nonlinear differential equations, and by automata, with discrete event dynamics behavior [14, 12]. The hybrid model is entirely described by the given following system [15,16,5]

$$H=\{Q, X, Init, f, X_q, E, G\}. \tag{5}$$

4.1. OPERATING MODE

Our system contains the discrete variables, which are the switches (supposedly perfect), each switch takes two values, 0 or 1. According to the state of the switches, the three-cell converter possesses 2^3 different configurations belonging to the set $Q=\{q_1, q_2, q_3, \ldots, q_8\}$. Each mode is defined in the space: $X_{qi}=R^3$, $\forall\ q_i \in Q$,

Here a continuous dynamic can be given for each mode of the following form:

$$fq(X)=A(q)X+b(q), \tag{6}$$

where X is the state vector of the system, grouping the state variables $X=[V_{c1}\ V_{c2}\ I\ w]^{\mathrm{T}}$.

The operating modes, as well as the system's dynamics, are given in the following Fig. 2 to Fig. 8.

Note. This is the eight modes of operation of a three cells converter with a continuous dynamic for each mode.

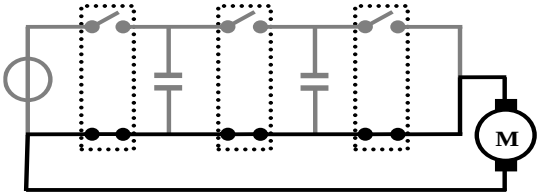

Fig. 2 – Mode $q = q_1$, with $\left(u = \left[u_1\, u_2\, u_3\right]^{\mathrm{T}} = \left[0\,0\,0\right]^{\mathrm{T}}\right)$.

$$f_{q1}(x) = \begin{bmatrix} 0 & 0 & 0 & 0 \\ 0 & 0 & 0 & 0 \\ 0 & 0 & -R/L & -K_e/L \\ 0 & 0 & K_c/J_m & -f_m/J_m \end{bmatrix} x + \begin{bmatrix} 0 \\ 0 \\ 0 \\ -C_r/J_m \end{bmatrix} \quad (7)$$

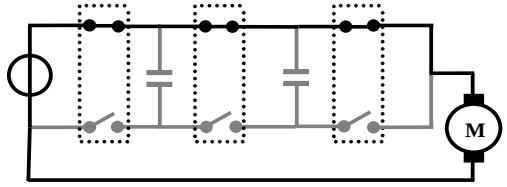

Fig. 3 – Mode $q = q_2$, with $\left(u = \left[u_1\, u_2\, u_3\right]^{\mathrm{T}} = \left[1\,0\,0\right]^{\mathrm{T}}\right)$.

$$f_{q2}(x) = \begin{bmatrix} 0 & 0 & -1/C_1 & 0 \\ 0 & 0 & 0 & 0 \\ 1/L & 0 & -R/L & -K_e/L \\ 0 & 0 & K_c/J_m & -f_m/J_m \end{bmatrix} x + \begin{bmatrix} 0 \\ 0 \\ 0 \\ -C_r/J_m \end{bmatrix} \quad (8)$$

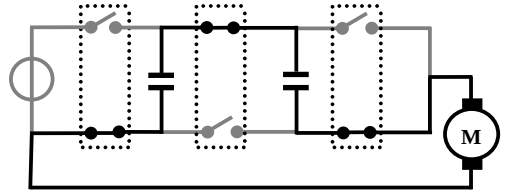

Fig. 4 – Mode $q = q_3$, with $\left(u = \left[u_1\, u_2\, u_3\right]^{\mathrm{T}} = \left[0\,1\,0\right]^{\mathrm{T}}\right)$.

$$f_{q3}(x) = \begin{bmatrix} 0 & 0 & 1/C_1 & 0 \\ 0 & 0 & 0 & 0 \\ -1/L & 1/L & -R/L & -K_e/L \\ 0 & 0 & K_c/J_m & -f_m/J_m \end{bmatrix} x + \begin{bmatrix} 0 \\ 0 \\ 0 \\ -C_r/J_m \end{bmatrix} \quad (9)$$

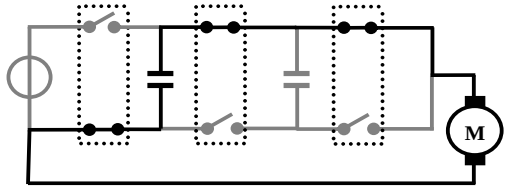

Fig. 5 – Mode $q = q_4$, with $\left(u = \left[u_1\, u_2\, u_3\right]^{\mathrm{T}} = \left[1\,1\,0\right]^{\mathrm{T}}\right)$.

$$f_{q4}(x) = \begin{bmatrix} 0 & 0 & 0 & 0 \\ 0 & 0 & -1/C_2 & 0 \\ 0 & 1/L & -R/L & -K_e/L \\ 0 & 0 & K_c/J_m & -f_m/J_m \end{bmatrix} x + \begin{bmatrix} 0 \\ 0 \\ 0 \\ -C_r/J_m \end{bmatrix} \quad (10)$$

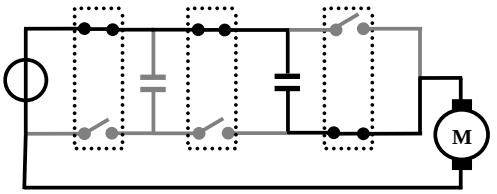

Fig. 6 – Mode $q = q_5$, with $\left(u = \left[u_1\, u_2\, u_3\right]^{\mathrm{T}} = \left[0\,0\,1\right]^{\mathrm{T}}\right)$.

$$f_{q5}(x) = \begin{bmatrix} 0 & 0 & 0 & 0 \\ 0 & 0 & +1/C_2 & 0 \\ 0 & -1/L & -R/L & -K_e/L \\ 0 & 0 & K_c/J_m & -f_m/J_m \end{bmatrix} x + \begin{bmatrix} 0 \\ 0 \\ E/L \\ -C_r/J_m \end{bmatrix} \quad (11)$$

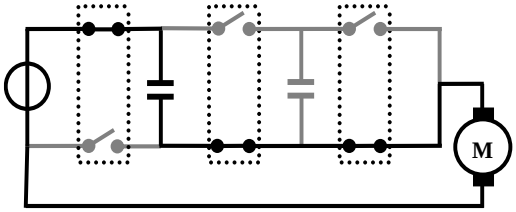

Fig. 7 – Mode $q = q_6$, with $\left(u = \left[u_1\, u_2\, u_3\right]^{\mathrm{T}} = \left[1\,0\,1\right]^{\mathrm{T}}\right)$.

$$f_{q6}(x) = \begin{bmatrix} 0 & 0 & -1/C_1 & 0 \\ 0 & 0 & +1/C_2 & 0 \\ 1/L & -1/L & -R/L & -K_e/L \\ 0 & 0 & K_c/J_m & -f_m/J_m \end{bmatrix} x + \begin{bmatrix} 0 \\ 0 \\ E/L \\ -C_r/J_m \end{bmatrix} \quad (12)$$

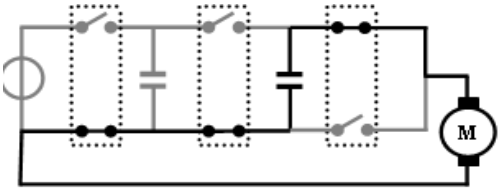

Fig. 8 – Mode $q = q_7$, with $\left(u = \left[u_1\, u_2\, u_3\right]^{\mathrm{T}} = \left[0\,1\,1\right]^{\mathrm{T}}\right)$.

$$f_{q7}(x) = \begin{bmatrix} 0 & 0 & 1/C_1 & 0 \\ 0 & 0 & 0 & 0 \\ -1/L & 0 & -R/L & -K_e/L \\ 0 & 0 & K_c/J_m & -f_m/J_m \end{bmatrix} x + \begin{bmatrix} 0 \\ 0 \\ E/L \\ -C_r/J_m \end{bmatrix} \quad (13)$$

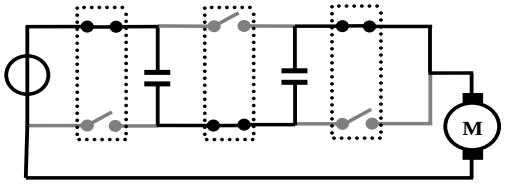

Fig. 9 – Mode $q = q_8$, with $\left(u = \left[u_1\, u_2\, u_3\right]^{\mathrm{T}} = \left[1\,1\,1\right]^{\mathrm{T}}\right)$.

$$f_{q8}(x) = \begin{bmatrix} 0 & 0 & 0 & 0 \\ 0 & 0 & 0 & 0 \\ 0 & 0 & -R/L & -K_e/L \\ 0 & 0 & K_c/J_m & -f_m/J_m \end{bmatrix} x + \begin{bmatrix} 0 \\ 0 \\ E/L \\ -C_r/J_m \end{bmatrix} \quad (14)$$

Knowing that one must control the voltages of the capacitors and the motor speed around the reference values as follows:

$$w = w_{ref}, \qquad V_{c1ref} = \frac{1}{3}E, \qquad V_{c2ref} = \frac{2}{3}E. \quad (15)$$

The hybrid control consists of choosing the suitable transitions between the different converter modes to achieve good performances. We must decide under what conditions the control sequence changes from one mode to another. We define the limits of state variables as follows:

$$\begin{gathered} \left(V_{c1ref}^{-} < V_{c1} < V_{c1ref}^{+}\right), \left(V_{c2ref}^{-} < V_{c1} < V_{c2ref}^{+}\right), \\ \left(w_{ref}^{-} < w < w_{ref}^{+}\right), \end{gathered} \quad (16)$$

such as:

$$V_{c1ref}^{+} = V_{cref} + \varepsilon \quad (17)$$

$$V_{c1ref}^{-} = V_{cref} - \varepsilon, \quad (18)$$

$$w_{ref}^{+} = w_{ref} + \Delta w, \quad (19)$$

$$w_{ref}^{-} = w_{ref} - \Delta w. \quad (20)$$

The transitions between the modes are then governed by these conditions; if one of them is violated during the operation of a given mode, the system should switch to another mode to find again the balance while respecting the

rule of adjacency. The possible conditions of the transitions between the various modes (considering the converter working conditions) satisfy the property described below:

$$G(q_1,q_2)= \left\{x\subset R^3:\left[\left(W<W_{ref}^-\right)\wedge\left(V_{c1}>V_{c1ref}\right)\wedge\left(V_{c2}>V_{c2ref}\right)\right]\right\} \quad (21)$$

$$G(q_2,q_1)=\left\{x\subset R^3:\left[\left(W>W_{ref}^+\right)\right]\right\} \quad (22)$$

$$G(q_1,q_3)= =\left\{x\subset R^3:\begin{bmatrix}\left(W<W_{ref}^-\right)\wedge\left(V_{c1}<V_{c1ref}\right)\wedge\\ \wedge\left(V_{c2}>V_{c2ref}\right)\end{bmatrix}\right\} \quad (23)$$

$$G(q_3,q_1)=\left\{x\subset R^3:\left[\left(W>W_{ref}^+\right)\right]\right\} \quad (24)$$

$$G(q_1,q_5)= =\left\{x\subset R^3:\begin{bmatrix}\left[\begin{bmatrix}\left(W<W_{ref}^-\right)\wedge\left(V_{c1}>V_{c1ref}\right)\wedge\\ \wedge\left(V_{c2}<V_{c2ref}\right)\end{bmatrix}\right]\\ \vee\left[\left(W<W_{ref}^-\right)\wedge\left(V_{c1}<V_{c1ref}\right)\right]\end{bmatrix}\right\} \quad (25)$$

$$G(q_5,q_1)= =\left\{x\subset R^3:\left[\left(W>W_{ref}\right)\wedge\left(V_{c2}>V_{c2ref}\right)\right]\right\} \quad (26)$$

$$G(q_2,q_4)= =\left\{x\subset R^3:\begin{bmatrix}\left(W<W_{ref}^+\right)\wedge\\ \wedge\left(V_{c1}>V_{c1ref}^-\right)\wedge\left(V_{c2}>V_{c2ref}^+\right)\end{bmatrix}\right\} \quad (27)$$

$$G(q_4,q_2)= =\left\{x\subset R^3:\begin{bmatrix}\left(W>W_{ref}\right)\wedge\left(V_{c1}>V_{c1ref}\right)\wedge\\ \wedge\left(V_{c2}>V_{c2ref}^-\right)\end{bmatrix}\right\} \quad (28)$$

$$G(q_3,q_4)= =\left\{x\subset R^3:\begin{bmatrix}\left[\begin{bmatrix}\left(W<W_{ref}^+\right)\wedge\left(V_{c1}>V_{c1ref}^+\right)\wedge\\ \wedge\left(V_{c2}<V_{c2ref}\right)\end{bmatrix}\right]\\ \vee\left[\left(W<W_{ref}^+\right)\wedge\left(V_{c2}<V_{c2ref}^-\right)\right]\end{bmatrix}\right\} \quad (29)$$

$$G(q_3,q_4)= =\left\{x\subset R^3:\begin{bmatrix}\left[\begin{bmatrix}\left(W<W_{ref}^+\right)\wedge\left(V_{c1}>V_{c1ref}^+\right)\wedge\\ \wedge\left(V_{c2}<V_{c2ref}\right)\end{bmatrix}\right]\\ \vee\left[\left(W<W_{ref}^+\right)\wedge\left(V_{c2}<V_{c2ref}^-\right)\right]\end{bmatrix}\right\} \quad (30)$$

$$G(q_4,q_3)= =\left\{x\subset R^3:\begin{bmatrix}\left(W<W_{ref}^+\right)\wedge\left(V_{c1}>V_{c1ref}^-\right)\wedge\\ \wedge\left(V_{c2}<V_{c2ref}^+\right)\end{bmatrix}\right\} \quad (31)$$

$$G(q_2,q_6)= =\left\{x\subset R^3:\begin{bmatrix}\left(W<W_{ref}^+\right)\wedge\left(V_{c1}>V_{c1ref}^-\right)\wedge\\ \wedge\left(V_{c2}>V_{c2ref}^-\right)\end{bmatrix}\right\} \quad (32)$$

$$G(q_3,q_7)= =\left\{\begin{matrix}x\subset R^3:\\ :\begin{bmatrix}\left[\left(V_{c1}>V_{c1ref}^+\right)\wedge\left(V_{c2}<V_{c2ref}\right)\wedge\left(W<W_{ref}^+\right)\right]\\ \vee\left[\left(V_{c1}<V_{c1ref}\right)\wedge\left(V_{c2}>V_{c2ref}^+\right)\wedge\left(W<W_{ref}^+\right)\right]\end{bmatrix}\end{matrix}\right\} \quad (33)$$

$$G(q_7,q_3)= =\left\{\begin{matrix}x\subset R^3:\\ :\begin{bmatrix}\left[\left(V_{c1}>V_{c1ref}^+\right)\wedge\left(V_{c2}>V_{c2ref}\right)\wedge\left(W>W_{ref}\right)\right]\\ \vee\left[\left(V_{c1}>V_{c1ref}^+\right)\wedge\left(V_{c2}>V_{c2ref}^+\right)\wedge\left(W<W_{ref}^+\right)\right]\end{bmatrix}\end{matrix}\right\} \quad (34)$$

$$G(q_4,q_8)= =\left\{x\subset R^3:\begin{bmatrix}\left[\begin{bmatrix}\left(W>W_{ref}\right)\wedge\left(V_{c1}<V_{c1ref}\right)\wedge\\ \wedge\left(V_{c2}<V_{c2ref}^-\right)\end{bmatrix}\right]\\ \vee\left[\left(V_{c2}<V_{c2ref}^-\right)\wedge\left(W<W_{ref}\right)\right]\end{bmatrix}\right\} \quad (35)$$

$$G(q_8,q_4)= =\left\{\begin{matrix}x\subset R^3:\\ :\begin{bmatrix}\left[\left(W>W_{ref}^+\right)\wedge\left(V_{c2}>V_{c2ref}\right)\right]\vee\\ \vee\left[\begin{bmatrix}\left(V_{c1}>V_{c1ref}\right)\wedge\left(V_{c2}>V_{c2ref}\right)\wedge\\ \wedge\left(W<W_{ref}^-\right)\end{bmatrix}\right]\end{bmatrix}\end{matrix}\right\} \quad (36)$$

$$G(q_5,q_6)= =\left\{x\subset R^3:\left[\left(V_{c1}>V_{c1ref}^+\right)\wedge\left(V_{c2}<V_{c2ref}\right)\right]\right\} \quad (37)$$

$$G(q_6,q_5)= =\left\{x\subset R^3:\left[\left(V_{c1}<V_{c1ref}^-\right)\wedge\left(V_{c2}<V_{c2ref}\right)\right]\right\} \quad (38)$$

$$G(q_5,q_7)= =\left\{x\subset R^3:\left[\left(W<W_{ref}\right)\wedge\left(V_{c2}>V_{c2ref}^+\right)\right]\right\} \quad (39)$$

$$G(q_7,q_5)= =\left\{x\subset R^3:\left[\left(V_{c1}>V_{c1ref}^+\right)\wedge\left(V_{c2}<V_{c2ref}\right)\right]\right\} \quad (40)$$

$$G(q_6,q_8)= =\left\{x\subset R^3:\left[\left(V_{c1}>V_{c1ref}^-\right)\wedge\left(V_{c2}>V_{c2ref}\right)\right]\right\} \quad (41)$$

$$G(q_8,q_6)= \left\{\begin{matrix}x\subset R^3:\\ :\begin{bmatrix}\left[\left(V_{c1}>V_{c1ref}\right)\wedge\left(V_{c2}<V_{c2ref}\right)\wedge\left(W>W_{ref}^+\right)\right]\\ \vee\left[\left(V_{c1}>V_{c1ref}\right)\wedge\left(V_{c2}<V_{c2ref}\right)\wedge\left(W<W_{ref}^+\right)\right]\end{bmatrix}\end{matrix}\right\} \quad (42)$$

$$G(q_7,q_8)= =\left\{x\subset R^3:\left[\left(V_{c1}>V_{c1ref}^+\right)\wedge\left(V_{c2}<V_{c2ref}\right)\right]\right\} \quad (43)$$

$$G(q_8,q_7)= =\left\{x\subset R^3:\begin{bmatrix}\left[\left(V_{c1}<V_{c1ref}\right)\wedge\left(W<W_{ref}^-\right)\right]\\ \vee\left[\left(V_{c1}<V_{c1ref}\right)\wedge\left(V_{c2}<V_{c2ref}\right)\wedge\left(W>W_{ref}^+\right)\right]\end{bmatrix}\right\} \quad (44)$$

Note. The other transitions (example: $G(q_1;q_4)$) are not tolerated because they do not comply with the adjacency rule.

The initial conditions of the system are defined by:

$$Init=\{q_8\}X\left\{\begin{matrix}x\in^3:\left[\left(V_{c1}<V_{c1ref}^-\right)\wedge\left(V_{c2}<V_{c2ref}^-\right)\right]\vee\\ \vee\left[\left(W<W_{ref}^-\right)\right]\end{matrix}\right\} \quad (45)$$

The dynamics of each mode are indicated inside each circle, and the conditions of transitions at the top from the

arrows $\left(\text{with } T_{ij} = G\left(q_i; q_j\right)\right)$ when a condition of transition is checked, the system commutates towards another mode [5].

5. EXPERIMENTATIONS

The implementation of the numerical control of the DC motor by controlling more cells of commutations is performed using Spartan 3E FPGA. It can calculate and send the desired signals to the control and power electronics, and it's specifically designed to meet the needs of high-volume, cost-sensitive consumer electronic applications. The five-member family offers densities ranging from 100,000 to 1.6 million system gates. To experimentally validate the commissioning of the converter, we build a test bench. The latter consists of multicellular arms in series with three cells; the switches of each arm are constituted of a MOSFET transistor connected antiparallel with the diodes. The MOSFETs are associated with command modules managing the dead times and protecting against short circuits. The MOSFET control signals are derived from a Xilinx Spartan 3E card. Figure 10 shows the realized test bench, and it is composed of:

- The power section includes the drivers, switches, and capacitors.
- The measurement part consists of voltage sensors and floating capacitors.
- The command part is made of a Spartan 3E FPGA control card and is computer-driven.

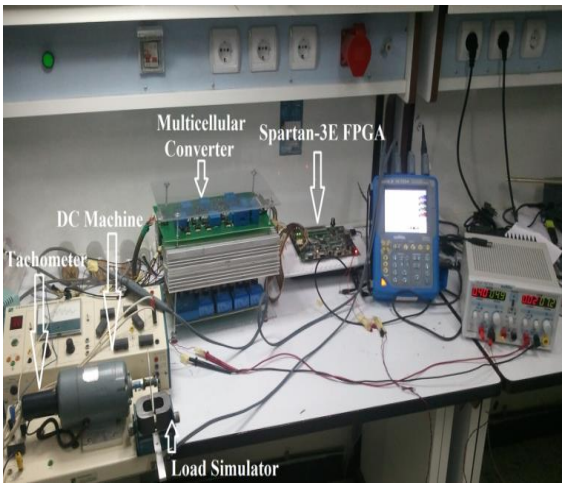

Fig.10 – A synopsis of the test bench carried out.

6. SIMULATION AND EXPERIMENTAL RESULTS

In this section, we present some simulation and experimental results obtained by using the proposed approach. To illustrate the performance of the proposed approach, we use hybrid control as an alternative to command the dc machine with a three-cell converter and make the simulation and experimental study.

Figures 11 and 12, respectively simulation and experimentally, show the evolution of the voltages V_{c1}, V_{c2} at the boundaries of the floating capacitors, the tension increase stabilizes around its reference value. Its average value is equal to one-third of the supply voltage E to the first capacitor and two-thirds for the second capacitor, where we notice the distribution of the voltage between the two capacitors both by simulation and experimentally.

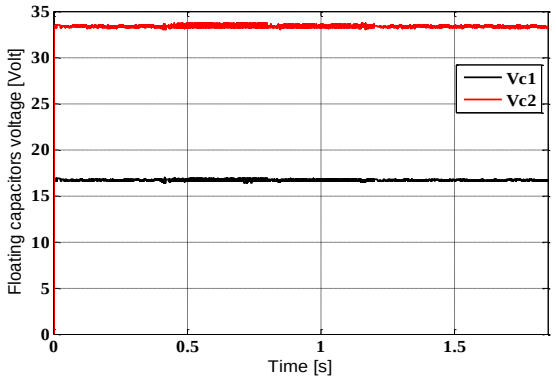

Fig. 11 – Evolution of the floating voltages V_{c1} and V_{c2} of the capacitors C_1 and C_2 – simulation test.

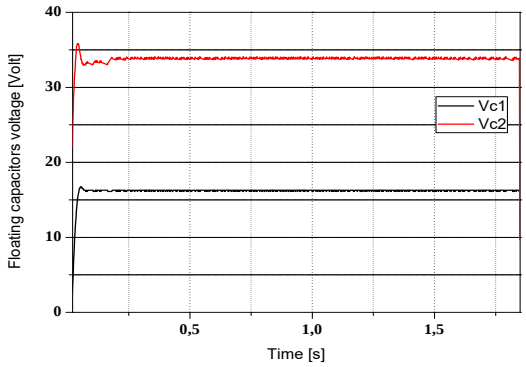

Fig. 12 – Evolution of the floating voltages V_{c1} and V_{c2} of the capacitors C_1 and C_2 – experimental test.

Figures 13 and 14, respectively experimentally and by simulation, show this command where we see clearly that the rotational speed follows its reference, despite the introduction of load torque and using multiple samples of speed references, with both simulation and experimentation.

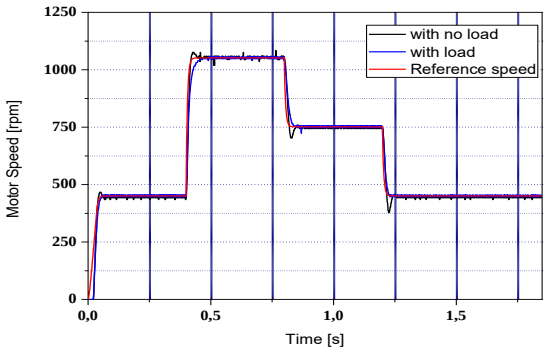

Fig. 13 – Evolution of the rotational speed and the reference speed – experimental test.

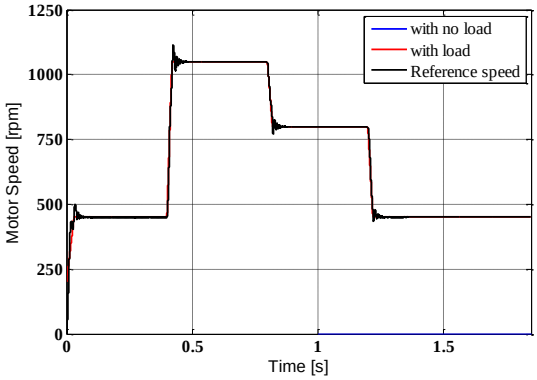

Fig. 14 – Evolution of the rotational speed and the reference speed – simulation test.

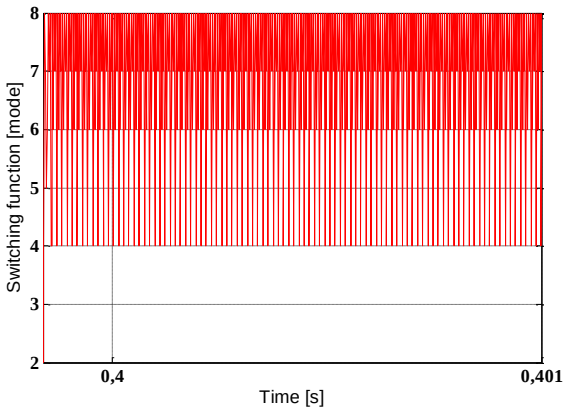

Fig. 15 – Evolution of switching function *Q*.

7. **STABILITY STUDY**

Consider our systems, $\mathrm{d}x/\mathrm{d}t = A_q x(t)$, $q \in \{q_1,..,q_n\}$, $n \in N$, is composed of different modes, such as $N = 8$ in our case, with the state matrices used in section 4.1. With the use of the Liberzon theorem, the stability of the switched system is proven with arbitrary switching signals, and a common quadratic Lyapunov matrix is found by convex optimization algorithms such as:

$$P = \begin{bmatrix} 0.0605 & 0.0896 & 0.6587 & 0.2581 \\ 0.0354 & 0.0605 & 0.2587 & 0.2541 \\ 0.0251 & 0.8746 & 6.0512 & 0.2541 \\ 0.2587 & 0.9870 & 0.2587 & 6.1058 \end{bmatrix}.$$

This algorithm is easily found in MATLAB with simple instructions in it.

8. **CONCLUSIONS**

In this work, the use of a multicellular converter to supply a dc machine has proven to be efficient both in theoretical terms as well as experimentally. We exploited this topology to ensure even distribution of voltage constraints on components' power.

Despite the introduction of the load and using multiple references of speed and implementation of several samples as references, the command used is characterized by better control of the transitional system of the machine, which leads to good response time and fast disturbance rejection. With a good choice of the actuator (dc) and a robust control (hybrid control), and with a good diet (Multicellular converter) like ours, we could check the first formula of our article. Therefore, our system can provide superior performance in terms of increased efficiency. The quadratic stability analysis for switched systems is more interesting than other methods since a cell partition, and a switching law will not affect the system's stability.

APPENDIX

The numerical parameters of the dc motor are $R = 1.44\,\Omega$, $L = 3.610^{-4}$ H, $J_m = 1.2910^{-4}$ kgm^2, $f_m = 5.1910^{-5}$ Nms**,** $k_t = 0.01$ Nm/A, $k_e = 0.01$ V/rad/s, $E = 12$ V, and the values of the capacitors of the inverter is $C_1 = C_2 = 1$ µF.

Received on 20 March 2019

REFERENCES

1. M.S Branicky, S.K. Mitter, *Algorithms for optimal hybrid control*, 34th IEEE Conference on Decision and Control (CDC95), New Orleans, pp. 2661-2666 (1995).
2 .T. Meynard, H. Foch, *Dispositif de conversion d'energie electrique a semiconducteur* Brevet Francais no. 91, 09582, Europe, Japan, USA, Canada, 92, 00652.
3. I. Bentchikou, F. Boudjema, D. Boukhetala, N.O. Cherchali, A. Tlemcani, *Investigation in the technique of adaptive predictive control fed by a hybrid inverter applied to a permanent magnet synchronous machine*, Nonlinear Dynamics and Systems Theory, **16** (2016).
4. A. Hagar, *Generalized multi-cell voltage sourced converter*, Power Electronics and Applications, (EPE '09), 13th European Conference on, pp. 1–6 (2009).
5. K. Benmansour, A. Benalia, M. Djemai, J. Leon, *Hybrid control of a multicellular converter*, Elsevier, Nonlinear Analysis: Hybrid systems, **1**, *1*, pp. 16–29 (2007).
6. T.A. Meynard, H. Foch, P. Thomas, J. Courault, R. Jakob, M. Nahrstaedt, *Multicell converters: basic concepts and industry applications*, IEEE Transactions on Industrial Electronics, **49**, pp. 955–964 (2002).
7. M.R. Skender, A. Tlemcani, *Implementation of a new super twisting ODE algorithm controlled by Dspace: application to series multicell converter*, Studies in Informatics and Control, **25**, *2* (2016).
8. S. Hanafi, M.K. Fellah, M.Yaichi, M.F.Benkhoris, *Nonlinear feedback decoupling control applied to stacked multicellular converter*", Rev. Roum. Sci. Techn. – Électrotechn. et Énerg., **59**, *1*, pp. 97-106 (2014)
9. B.C. Florea, D.A. Stoichescu, A. Spataru, *A direct control method for multicellular converters*, U.P.B. Sci. Bull., Series C, **74**, *3* (2012) .
10. D. Patino, P. Riedinger, C. Iung, *Predictive control approach for multicellular converters*, Industrial Electronics (IECON 2008), 34th Annual Conference of IEEE, pp. 3309-3314.
11. J. S. Lai and F. Z. Peng, *Multilevel converters-a new breed of power converters*, IEEE Transactions on Industrial Applications, **32**, *3*, pp. 2348 – 2356 (1996).
12. O. Benzineb, F. Taibi, T. M. Laleg-Kirati, M. S. Boucherit, M.Tadjine, *Control and fault diagnosis based sliding mode observer of a multicellular converter: hybrid approach*, J. of Electrical Engineering, **64**, *1*, pp. 20-30 (2013).
13. P. Lezana, R. Aguilera, J. Rodriguez, *Fault detection on multicell converter based on output voltage frequency*, Analysis, Industrial Electronics, IEEE Transactions on, **56**, *6*, pp. 2275–2283 (2009).
14. V. DargahiA, M. Barzadeh, A. Darvishi, M. Salehifar, A.Shoulaie, *Voltage compensation by a modified mixed cascade flying capacitor multicell inverter*, Power Quality Conference (PQC), p. 5 (2010).
15. J. Lygeros, K.H Johansson, S.N. Simie, S.S. Sastry, *Dynamical properties modeling of hybrid automata*, IEEE Transactions on automatic control, **48,** January 2003.
16. M.R. Skender, A. Tlemcani, *Nouvel algorithme d'observation à mode glissant d'ordre supérieur appliqué au convertisseur multicellulaire série*, Rev. Roum. Sci. Techn.– Électrotechn. et Énerg., **61**, *2*, pp. 126–130 (2016).
17. R. Stella, S. Pirog, M. Baszynski, A. Mondzik, A. Penczek, J. Czekonski, S. Gasiorek, *Results of investigation of multicell converters with balancing circuit*. Part I, Industrial Electronics, IEEE Transactions on, **56**, *7*, pp. 2610-2619 (2009).